buildings

MDPI

Article

Strength and Microstructural Changes in Cementitious Composites Containing Waste Oyster Shell Powder

Min Ook Kim [1,*] and Myung Kue Lee [2]

[1] Department of Civil Engineering, Seoul National University of Science and Technology, 232 Gongneung-ro, Nowon-gu, Seoul 01811, Republic of Korea
[2] Department of Civil and Environmental Engineering, Jeonju University, 303 Cheonjam-ro, Wansan-gu, Jeollabuk-do, Jeonju 55069, Republic of Korea; concrete@jj.ac.kr
* Correspondence: minookkim@seoultech.ac.kr; Tel.: +82-2-970-6514

Abstract: In this study, the effect of adding waste oyster shell powder (WOSP) on the strength and microstructure of cementitious composites was experimentally investigated. The test variables included the WOSP replacement ratios (0, 25, 50, and 75%) by weight of cement, the type of curing water (tap water and seawater), and the curing period (7, 28, 90, 180, and 365 d). The compressive strength, flexural strength, and initial and secondary sorptivity were measured at specific ages. Moreover, scanning electron microscopy (SEM) and X-ray diffraction (XRD) measurements were conducted, and their results were analyzed. Samples with WOSP replacement ratios greater than 25% exhibited a rapid reduction in measured strength values. The correlation between compressive strength and initial sorptivity tends to be slightly higher than that between flexural strength and initial sorptivity. The one-year investigation revealed that there was no significant effect of using different curing waters on strength development. The effect of the curing period was evident in enhancing the strength only in the early stages, with no significant increase in strength observed after 28 d. The XRD analysis revealed that most samples prepared with WOSP contained $CaCO_3$, and the peak of $CaCO_3$ tended to increase with an increasing WOSP replacement ratio. The SEM results revealed that a high replacement ratio of WOSP can have a negative influence on cement hydration and the pozzolanic effect. The limitations of this study and future work were also discussed.

Keywords: waste oyster shell; strength; microstructure; cementitious composites; marine concrete structures

Citation: Kim, M.O.; Lee, M.K. Strength and Microstructural Changes in Cementitious Composites Containing Waste Oyster Shell Powder. *Buildings* **2023**, *13*, 3078. https://doi.org/10.3390/buildings13123078

Academic Editors: Marek Dohojda and Olga Szlachetka

Received: 16 November 2023
Revised: 4 December 2023
Accepted: 8 December 2023
Published: 11 December 2023

1. Introduction

Cement production releases substantial amounts of CO_2 into the atmosphere [1–5]. CO_2, generated during the process of heating limestone to produce clinker, can accelerate climate change and global warming as a greenhouse gas [6–9]. Cement factories emit air pollutants such as sulfur dioxide (SO_2) and nitrogen oxides (NO_x), which, when present in high concentrations in the atmosphere, can lead to health problems and ecosystem pollution [10–13]. Consequently, cement production can lead to the destruction of natural environments and ecosystems; this emphasizes the need to reduce cement consumption by using alternative resources [14–19]. The use of alternative materials to replace cement is essential for promoting environmental protection and sustainability in the construction industry. These alternative materials that typically partially or fully substitute for cement offer numerous advantages, including the reduction in CO_2 emissions associated with cement production, resource conservation, improved waste management, and enhanced durability [20–22]. Some well-known cement substitute materials include fly ash (FA) and silica fume (SF). Recently, novel alternative materials such as limestone, volcanic ash, and recycled plastics have been researched for creating sustainable concrete mixtures [23–27].

In South Korea, waste oyster shells (WOS) have become an urgent problem that needs to be addressed because of the excessive amount produced every year compared with the

limited storage space available. Approximately 300,000 tons of oyster shells are annually produced, which translates to a minimum of 300 kg of oyster shells generated every day [28]. WOS can negatively influence marine ecosystems if collected from polluted areas or if contaminated with harmful substances. Oyster shells mainly consist of $CaCO_3$ and have been widely used in agriculture and habitat restoration [29–32]. Similarly, they can be used in concrete as fillers to restore pores within concrete and improve its material properties.

Several studies have been conducted to investigate the effects of adding waste oyster shell powder (WOSP) as a replacement for fine aggregate or cement on the mechanical properties and durability of concrete [33–40]. These efforts aim to successfully recycle WOS and contribute to sustainable construction practices. Yang et al. investigated the effects of WOSP addition on the short- and long-term properties of concrete and reported that the strength gain at an early age was unaffected by WOSP addition [33,34]. However, there was no further increase in strength at long-term ages compared with the control sample. They also examined the effect of WOSP on concrete durability and observed improved resistance to freezing and thawing as well as reduced water permeability. Similarly, Kuo et al. confirmed that a WOSP replacement ratio of less than 20% did not show a significant difference in compressive strength compared with the control sample, and they concluded that WOSP was effective in replacing fine aggregates [35]. They also reported reduced water absorption with the addition of WOSP and suggested an optimal replacement rate of 5% for its application in construction. Liu et al. investigated the changes in the properties of cement mortar containing WOSP and reported that the use of polyvinyl alcohol as a pretreatment was effective in improving durability [36]. Overall, it can be observed that a replacement ratio of less than 20% might contribute to early strength gain, whereas a replacement ratio of more than 20% can lead to a significant reduction in strength. Bamigboye et al. investigated the feasibility of seashells as binders in concrete casting [37]. They concluded that the compressive strength can be reduced by adding seashells, and that a replacement ratio higher than 50% can have a negative influence on workability. Soltanzadeh et al. indicated that increasing the WOSP replacement ratio can lead to reduced strength because of the lower reactivity of WOSP compared with ordinary Portland cement [38]. They also noted that WOSP with a small particle size can function as a filler, filling the voids between the aggregate and cement paste. Han et al. reported a 45% reduction in the compressive strength of cement mortar when 30% of the cement was replaced with WOSP [39]. Seifu et al. concluded that WOSP can be used to fill inner pores, resulting in the formation of monocarbonates and hemicarbonates during the hydration process. This, in turn, contributes to the stability of ettringite [40]. Table A1 lists the reported compressive strengths of cementitious composites with various waste shell powder (WSP) replacement ratios [41–48]. The compressive strength values measured at 28 days varied depending on the type of shell and replacement ratios. This emphasizes the importance of conducting further studies to better utilize WOSP in cementitious composites.

Microstructural changes, such as the hydration process and pore structures, caused by the addition of WOSP to cementitious composites are of significant concern because they can influence both strength development and durability [39,49–51]. Han et al. indicated that the use of WOSP can accelerate cement hydration, and this trend was observed during the early stages, likely within the first day [39]. Similarly, this acceleration can contribute to an early strength gain, whereas the later strength may be reduced. Liu et al. reported that the incorporation of WOSP, with a mesh size of 3000 μm, can lead to dense microstructures in cement mortar, reducing both the total pore volume and the diameter size [49]. Liao et al. confirmed that the incorporation of WOSP resulted in a better pore distribution, as revealed by mercury intrusion porosimetry (MIP) tests [50]. Chen et al. conducted a comprehensive investigation to clarify the effects of different supplementary cementitious materials (SCMs), including FA and ground granulated blast furnace slag, on the material properties of crushed oyster shell mortar [51]. They reported a retarded hydration process when SCMs were used, particularly at an early age. WOSP is generally considered an inert material; thus, the inclusion of other pozzolanic materials is necessary to render it

functional in cementitious composites. The particle size of WOSP plays a significant role in the microstructures of cementitious composites. However, the performance can vary based on several factors, including the type of shell, pretreatment, and presence of SCMs.

To enable massive consumption of WOSP, discovering various applications using the developed optimal mix ratio is necessary. One possible application for the effective utilization of WOSP is in marine concrete structures, such as the production of artificial concrete reefs [52–54]. Kong et al. studied the feasibility of adding WOSP to produce porous concrete to create an artificial reef. They reported that the amount of WOSP was a key factor in determining the mechanical properties, durability, and alkalinity [52]. Klathae investigated the possibility of using WOSP as a cement replacement to produce interlocking blocks. To ensure appropriate mechanical properties, the replacement ratio should not exceed 20% [53]. Xu et al. conducted a field test to investigate the environmental effects of artificial reefs produced with WOSP and reported slightly improved quality based on short-term monitoring [54]. However, in marine applications, the impact of seawater on strength development and microstructural changes should be clearly understood. This is crucial because seawater contains harmful ions, including chloride ions, which can negatively influence the performance of concrete. Choi et al. compared the early-age mechanical properties of mortar samples exposed to either conventional tap water or seawater conditions [55]. They reported the positive effect of seawater, showing early strength gain and improved durability. They also highlighted the additional hydration caused by seawater, which can fill the pores ranging between 50 and 200 μm. However, Park et al. confirmed the retarded cement hydration rate in mortar samples containing various SCMs exposed to seawater [56]. The effects of seawater on the strength development and durability changes in cementitious composites are controversial, and an experimental investigation must be conducted prior to their application in marine environments.

Numerous studies have been conducted to enhance the use of WOSP in cementitious composites. However, further research is still essential for a more effective utilization of WOSP, and long-term investigations to monitor changes in the mechanical properties are required. Notably, the situation regarding WOSP can significantly vary depending on the region, country, and environmental conditions. In this regard, we experimentally examined the effects of WOSP, collected and prepared in South Korea, on the strength development and microstructural changes in cementitious composites exposed to different water conditions.

2. Research Significance

Numerous experimental studies have been conducted to investigate the feasibility of using WOSP in cementitious composites to reduce waste materials and promote sustainable construction. However, the mechanical properties of samples containing WOSP can significantly vary depending on the replacement ratio and the curing period. Additionally, utilization of waste oyster shells can differ depending on the region and country. Therefore, in this study, an experimental program was designed, and a comprehensive investigation was conducted to explore the crucial factors influencing the strength and microstructure of cementitious composites produced from WOSP. These factors include the WOSP replacement ratio, the curing age, and curing conditions. This research is part of an ongoing project focused on recycling WOSP in marine concrete structures such as in applications related to floating renewable energy systems, breakwaters, and artificial reefs. It is expected to provide a solution for the better utilization of WOSP considering its long-term properties.

3. Materials and Methods

Figure 1 summarizes the test variables and methods used in this study. These variables include different WOSP replacement ratios, curing water types, and curing ages. The measured values included compressive strength, flexural strength, and sorptivity (both initial and secondary). Additionally, X-ray diffraction (XRD) and scanning electron microscopy

(SEM) analyses were conducted on representative samples. Detailed information on the selected materials, test variables, and test procedures is provided in the following sections. To simplify the test analysis, samples were denoted using nomenclature. For example, 'W50-TW-90D' denotes a mortar sample in which 50% of the cement is replaced with WOSP by weight and cured under tap water for 90 d.

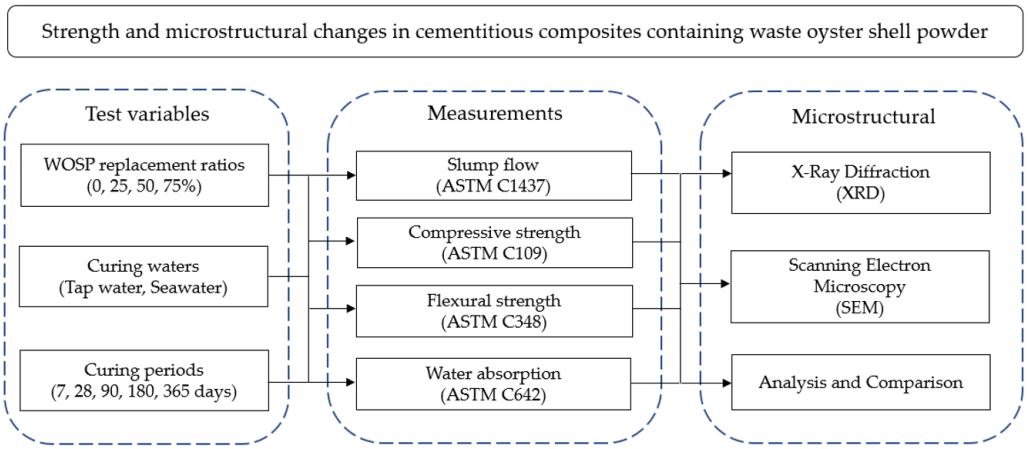

Figure 1. Test variables and methods selected in this study.

3.1. Materials and Sample Preparation

As summarized in Table 1, Type I ordinary Portland cement (OPC; Chunma Cement, Seoul, South Korea), SF (Elkem 940U; Elkem, Oslo, Norway), and WOSP were used to prepare the samples. WOSP was sourced from a local company that recycles oyster shells. Dried silica sand (ACS Corporation, Seoul, Republic of Korea) and a polycarboxylate-based high-range water-reducing superplasticizer (SP, Flowmix 3000 U; Dongnam, Gyeonggi-do, Republic of Korea) were used. Figure 2a–c show the SEM images, whereas Figure 3a,b show the particle size distributions and XRD results of the raw materials. The XRD pattern of SF showed a diffuse band at 15–30° corresponding to amorphous silica, while that of WOSP showed peak at 29.5° due to the presence of calcium carbonate. Table 2 lists the mix proportions used to prepare the samples, which replaced 0, 25, 50, or 75% of the cement weight at a constant water-to-binder (w/b) ratio of 0.36. Table 3 lists the chemical compositions of the tap water and seawater used for curing.

Table 1. Chemical characteristics (in mass- %) of raw materials.

Constituent (%)	OPC	SF	WOSP
CaO	61.40	1.54	85.12
SiO_2	21.23	96.90	1.78
Al_2O_3	5.64	0.29	0.31
Fe_2O_3	3.38	0.15	0.41
MgO	2.20	0.18	0.32
SO_3	2.25	–	1.01
K_2O	1.15	0.64	0.12
Na_2O	0.11	0.16	5.31
Cl	0.06	–	0.24
MnO	–	0.03	–
P_2O_5	–	0.05	0.19
Loss of Ignition	2.58	0.05	5.19

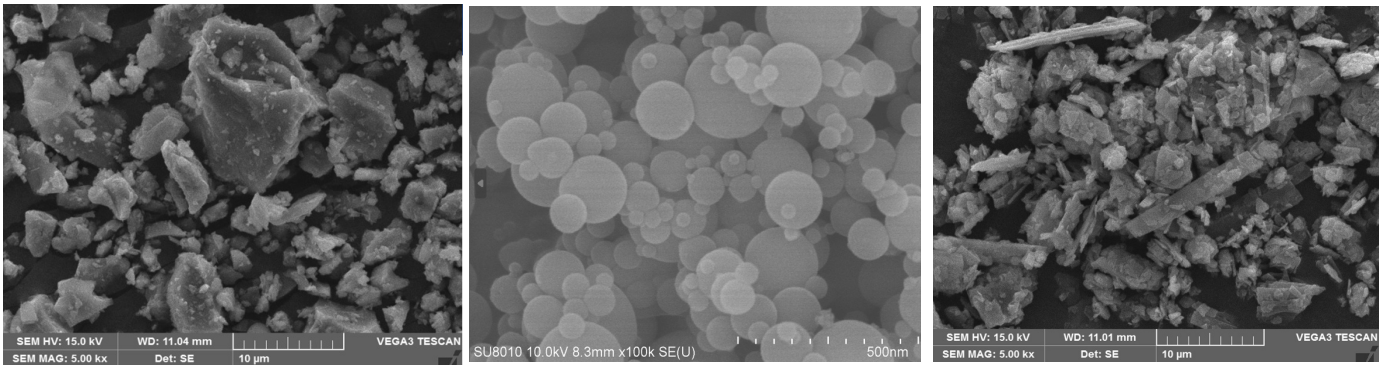

(**a**) (**b**) (**c**)

Figure 2. SEM images of raw materials (**a**) OPC, (**b**) SF, and (**c**) WOSP.

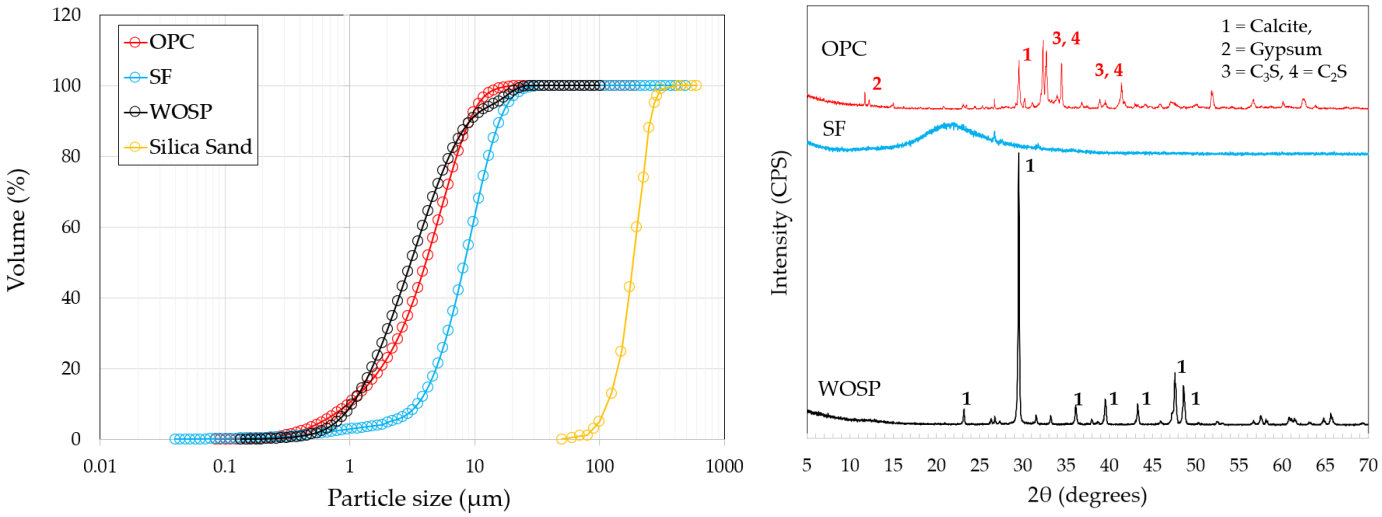

(**a**) (**b**)

Figure 3. (**a**) Particle size distributions and (**b**) XRD patterns of raw materials.

Table 2. Mix proportions of mortar samples (weight % of cement).

ID	OPC	SF	WOSP	Silica Sand	Water	SP	Flow (mm)
C100W0	1	0.25	-	1.45	0.45	0.012	235.0
C75W25	0.75		0.25				217.5
C50W50	0.50		0.50				180.0
C25W75	0.25		0.75				178.5

Table 3. Chemical compositions of tap water and seawater used in this study.

Ions	Tap Water (mg/L [1])	Seawater (mg/L)
Chloride (Cl^-)	39.1	21,075
Sodium (Na^+)	86.2	17,075
Sulfate (SO_4^{2-})	58.8	2258
Magnesium (Mg^{2+})	–	973
Calcium (Ca^{2+})	–	364
Potassium (K^+)	–	549
Nitrate (NO_{3-})	16.1	–

[1] mg/L = ppm, 1% = 10,000 ppm.

Table 4 includes pH, salinity, and temperature of tap water and seawater. pH was measured using a digital pH meter (Testo SE & Co., Seoul, Republic of Korea). Seawater used for curing was obtained from Yeongdeok, Republic of Korea. All the prepared raw materials were placed in a mixing pan considering the densities of the raw materials, and dry mixing was conducted for 3 min. Subsequently, water and SP were added, and the mixture was stirred for an additional 4 min. The mixing procedure adopted in this study was determined based on our previous study, considering both suitable workability and ensuring a high WOSP replacement relative to the weight of cement [40]. Prepared samples were cured in tap water under constant conditions of 20 °C and 60% relative humidity (RH) until the age of testing. The samples cured in seawater were placed in a moist chamber maintained at 20 ± 2 °C and 90–95% RH. Cubical specimens with dimensions of 50 mm × 50 mm × 50 mm, cylindrical specimens with dimensions of D100 mm × H200 mm, and beam specimens with dimensions of 40 mm × 40 mm × 160 mm were prepared for each mixed group. After one day of casting, the samples were removed from the molds and placed in a chamber at constant temperature and humidity. After the designated curing period, the tests were performed, and each measurement was conducted at least three times.

Table 4. pH, salinity, and temperature of tap water and seawater.

Type of Water	pH		Salinity (%)		Temperature (°C)	
	Mean	SD	Mean	SD	Mean	SD
Tap water	7.11	1.12	0.07	-	21.70	0.69
Seawater	8.35	0.19	2.56	0.21	20.50	0.51

3.2. Testing and Measurements

The compressive strength, flexural strength, and sorptivity of the mortar samples were measured following the standards outlined in ASTM C109, ASTM C348, and ASTM C1585, respectively [57–59]. The compressive and flexural strength measurements were conducted using a hydraulic universal testing machine (UTM) at constant loading rates of 900 N/s and 0.02 mm/min, respectively. The cylindrical specimens cured under different water conditions were removed from the chamber and cut to a height of 50 mm for the sorptivity test. Subsequently, the side of the sliced specimen was sealed with epoxy to prevent water exposure, and the top of the specimen was covered with a thin plastic sheet to prevent water evaporation during testing. The compressive and flexural strengths were calculated as follows:

$$f'_c = P_{max}/A, \quad (1)$$

where P_{max} pmax is the maximum force (N), and A is the contact area (=2500 mm^2) of the cubical specimen.

$$f'_b = P_{max}l/bd^2, \quad (2)$$

where P_{max} is the maximum force (N), l is the span length (mm), b is the width (mm), and d is the height (mm) of the flexural specimen. Sorptivity was estimated using the following equation:

$$I = m_t/ad, \quad (3)$$

where m_t is the mass of the sample measured at each time interval (g), a is the area exposed to water (mm^2), and d is the density of water (g/mm^3). The initial and secondary sorptivities were estimated based on slopes from 1 min to 6 h and 1 to 7 d, respectively.

XRD (Bruker DE/D8 Advance, Bruker, Germany) was used to investigate the phase compositions of the mortar samples containing different proportions of WOSP. The prepared samples were scanned within the range of 2θ between 5° and 70° at a scan speed of 0.02° and 0.3° per second using 45 kV voltage and 40 mA current. SEM images were captured using a TESCAN VEGA3 microscope (Tescan Korea, Seoul, Republic of Korea).

These images were then analyzed to investigate the phase change in the cementitious composites resulting from the weight-based replacement of cement with WOSP.

3.3. Analysis

The test results were analyzed using statistical analysis, and *p*-values were obtained. The one-way analysis of variance (ANOVA) test was used to confirm the effect of different curing water conditions on the strength development of the samples, with the null hypothesis implying no significant difference in strength between the samples. Compressive and flexural strength development ratios (SDR_c and SDR_f), normalized based on the strength at 365 d, were estimated to investigate the effect of the test variables on the strength changes. XRD and SEM images of representative samples were used to support the conclusions for each test variable.

4. Test Results

4.1. Compressive Strength

Figure 4 summarizes the measured mean compressive strengths and standard deviations (SDs). The maximum mean strength value was 48.12 MPa, with an SD of 2.18 MPa (W0-TW-365D), while the minimum strength value was 5.19 MPa, with an SD of 0.25 MPa (W75-TW-7D). The samples exposed to seawater conditions exhibited a 9% higher variation in the mean compressive strengths compared with those exposed to tap water. This difference may be attributed to the chemical composition of the seawater. The high variation in samples exposed to seawater was consistent with previous results showing a 14% increase, as reported by Choi et al. [55]. It should be noted that the difference in variation becomes more significant with higher WOSP replacement ratios. For instance, the differences in the SDs between tap water and seawater at 50 and 75% WOSP replacement ratios were 47 and 82%, respectively. A detailed analysis, comparison, and effect of the test variables on the measured values are discussed in the following sections.

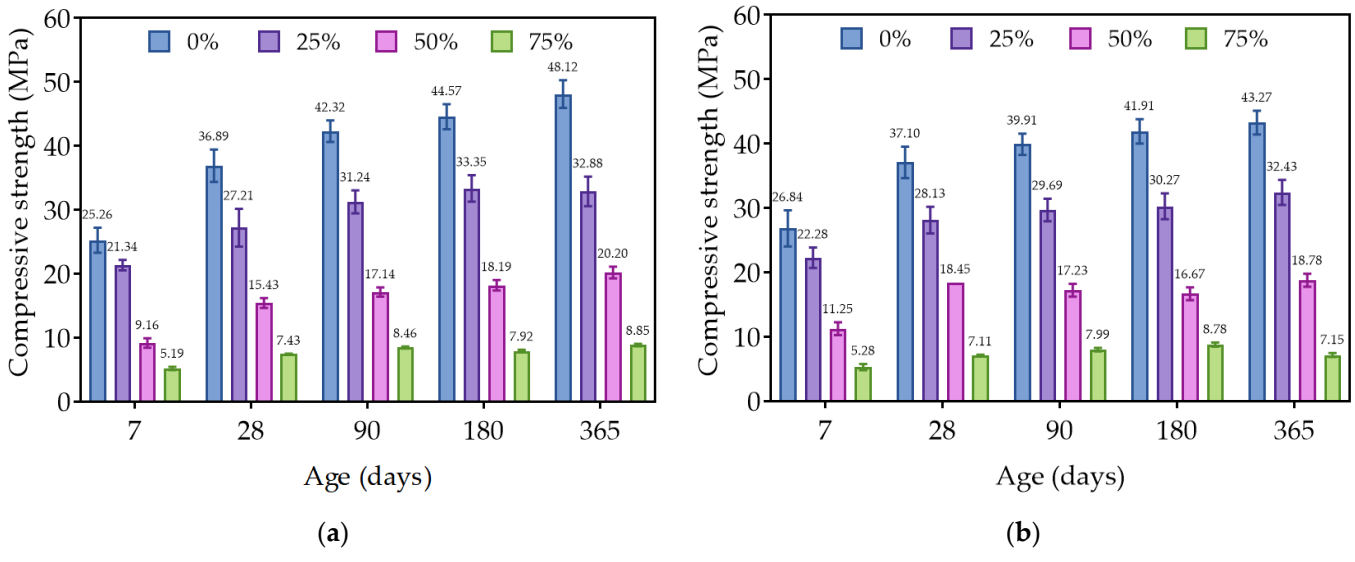

Figure 4. Compressive strength values of samples exposed to (**a**) tap water and (**b**) seawater.

4.2. Flexural Strength

Figure 5 presents the measured flexural strengths and SDs. The maximum mean flexural strength value was 9.77 MPa, with an SD of 0.67 MPa (W0-SW-90D), while the minimum strength was 2.05 MPa, with an SD of 0.32 MPa (W75-SW-7D). In the case of flexural strength, the difference in variation between the samples under the TW and SW conditions was only 4%. However, similar to the compressive strength results, the difference in SDs became significant with increasing WOSP replacement ratios. For example,

samples that included 75% WOSP and were cured under SW conditions exhibited a 29% higher average SD than samples cured under TW conditions. Figure 6 illustrates the relationship between the measured compressive and flexural strengths under various curing water conditions.

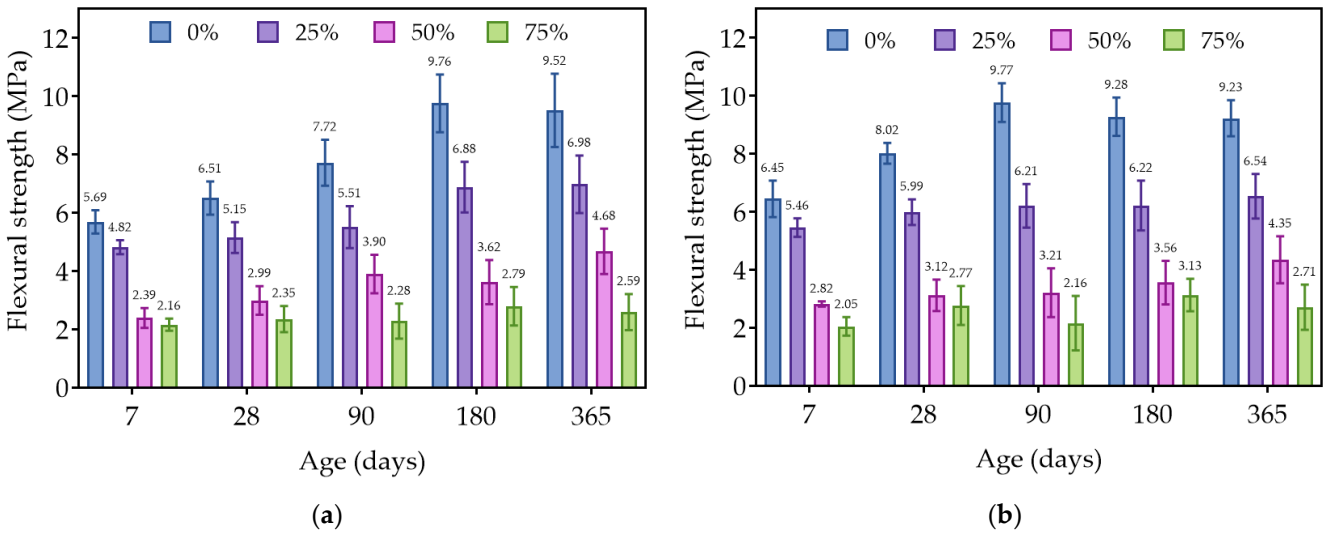

Figure 5. Flexural strength values of samples exposed to (**a**) tap water and (**b**) seawater.

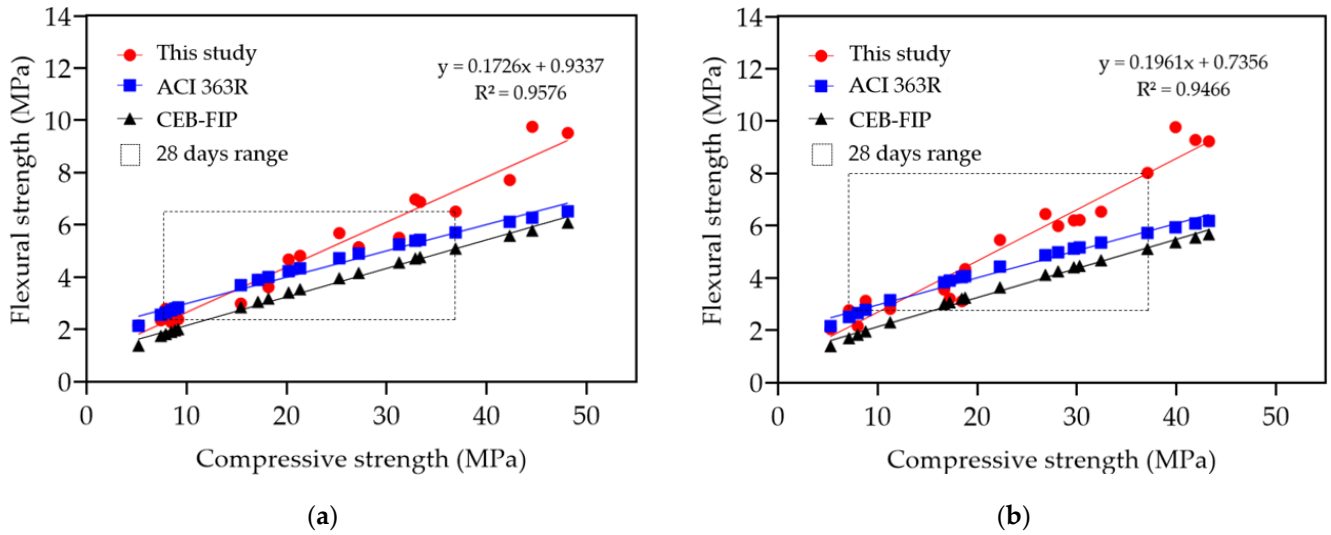

Figure 6. Relationship between compressive strength and flexural strength: (**a**) tap water condition and (**b**) seawater condition.

The values calculated according to ACI 363R and CEB-FIP are also shown in Figure 6 for comparison [60,61]. A strong correlation between the two strength values was observed, with high R-values (0.9576 and 0.9466) based on the linear regression for both conditions. The measured values in this study generally surpassed the values estimated from ACI 363R and CEB-FIP, particularly for the strengths measured at later ages. However, the values aligned well within those at 28 d under TW conditions.

4.3. Sorptivity

Figure 7a–d show the changes in the measured initial and secondary sorptivities for the curing period. Under conventional TW conditions, the initial sorptivity ranged from 0.057 to 0.325 mm/min$^{0.5}$, while the subsequent sorptivity ranged from 0.005 to 0.058 mm/min$^{0.5}$.

In SW conditions, the initial sorptivity ranged from 0.05 to 0.275 mm/min$^{0.5}$, and the secondary sorptivity ranged from 0.005 to 0.042 mm/min$^{0.5}$. The SW conditions exhibited smaller variations in the measured sorptivity than the TW conditions. Furthermore, the TW conditions showed a stronger correlation between the measured sorptivity and curing age than the SW conditions. In this study, we focused on using the initial sorptivity rather than the secondary sorptivity to examine the effects of the test variables and conducted further analysis. In this study, the R^2 values for the relationships between strength and initial sorptivity were generally low as shown in Figure 8. However, the correlation between compressive strength and initial sorptivity tends to be slightly higher than that between flexural strength and initial sorptivity.

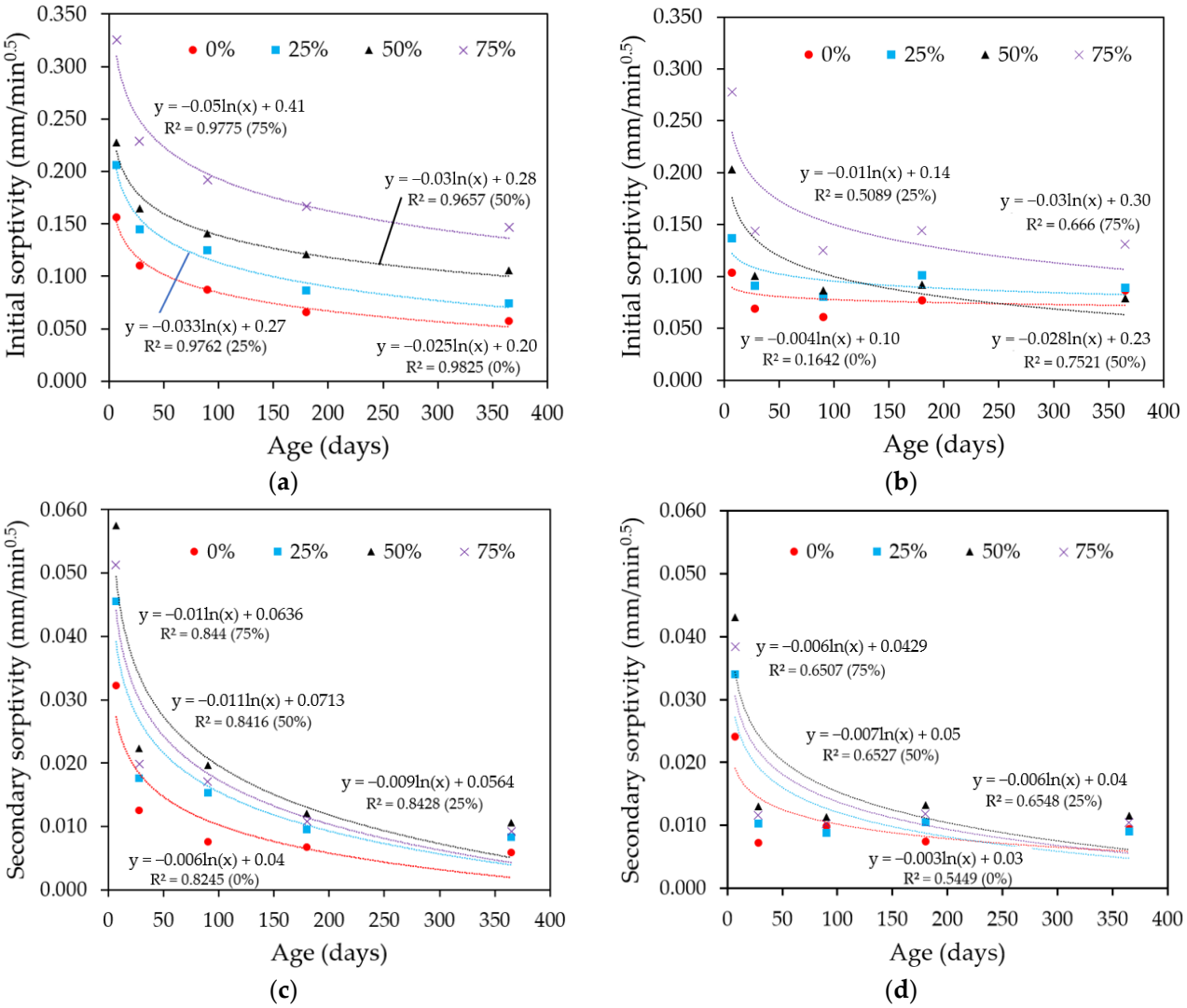

Figure 7. Measured sorptivity values: (**a**) initial sorptivity at TW condition, (**b**) initial sorptivity at SW condition, (**c**) secondary sorptivity at TW condition and (**d**) secondary sorptivity at SW condition.

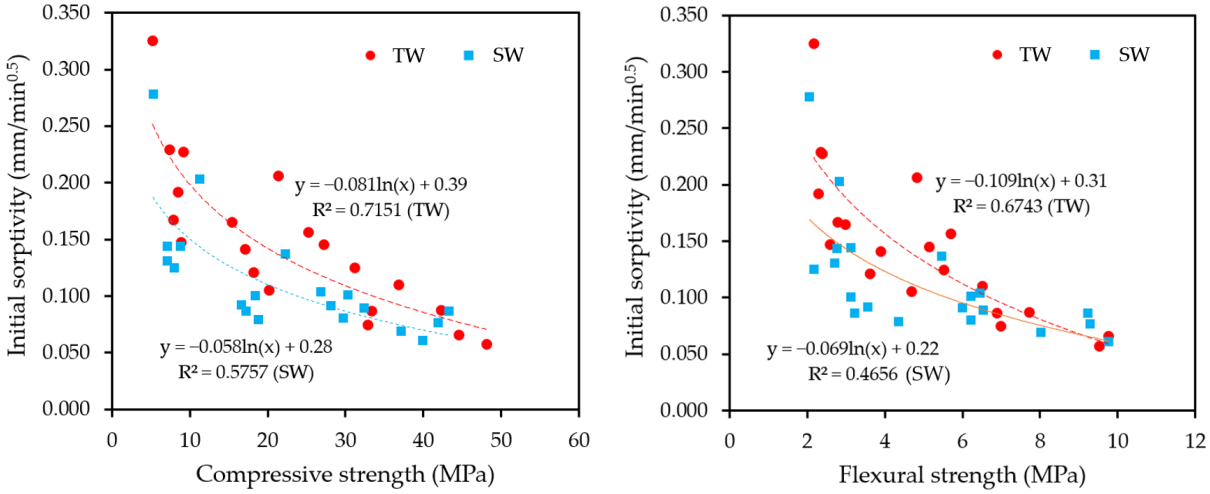

(**a**) (**b**)

Figure 8. Relationships between strength and initial sorptivity: (**a**) compressive strength and (**b**) flexural strength.

5. Analysis

5.1. Effect of WOSP Replacement Ratio on the Strength and Microstructures of Cementitious Composites

As expected, an increase in the WOSP replacement ratio resulted in a corresponding decrease in strength values, and this trend became more pronounced beyond a 25% replacement ratio. With an increase in the WOSP replacement ratio from 25 to 75%, the 28 d compressive strength was reduced by more than 70%, and the 28 d flexural strength decreased by approximately 54%, regardless of the curing conditions. These results are consistent with those of previous studies reporting a significant reduction in strength with replacements exceeding 50% [37,39]. Figures 9 and 10 show the effects of varying the WOSP replacement ratios on SDR_c and SDR_f of the samples exposed to TW and SW, respectively. In both figures, the spacing is arranged in the order of high-strength development from bottom to top, rather than by age, to facilitate better comprehension. Overall, the samples incorporating WOSP exhibited similar or higher SDR_c and SDR_f values than the control samples, particularly during the initial seven days. However, samples with higher WOSP content displayed an irregular increasing trend in strength development compared with the control sample. Additionally, both SDR_c and SDR_f increased when the WOSP-containing samples were cured under seawater conditions, implying that an appropriate curing procedure is crucial for achieving the anticipated strength before exposure to marine environments. Figure 11 shows the failure modes used to select the representative samples. Samples with higher WOSP replacement ratios exhibited more brittle failures, resulting in a lower maximum strength. This observation can also be attributed to the lower reactivity of the samples containing higher WOSP, as previously discussed [38]. Figure 12 shows the SEM images captured at 28 d for representative samples (W0-TW-28D, W25-TW-28D, W75-TW-28D, W0-SW-28D, W25-SW-28D, and W75-SW-28D), confirming a previously identified trend of low reactivity with more WOSP replacement. Based on a comparison of the SEM images, it can be observed that the samples with a higher WOSP replacement ratio exhibited lower reactivity than the control sample. Therefore, the function of WOSP as a filler in cementitious composites was not activated owing to its excessive powder content. That is, an excessively high inclusion of WOSP can disrupt its intended role, leading to a reduction in strength. The absence of WOSP leads to denser microstructures, which is in line with previous findings [62,63]. Overall, it can be concluded that a high WOSP replacement ratio can negatively influence strength development owing to reduced reactivity. WOSP contains calcium carbonate, which contributes to the material properties of the cementitious composites. For example, finely ground WOSP can act as a supplementary

cementitious material by reacting with cement hydration products and contributing to the strength and durability of cementitious composites. However, the use of WOSP beyond certain limits can significantly reduce the strength.

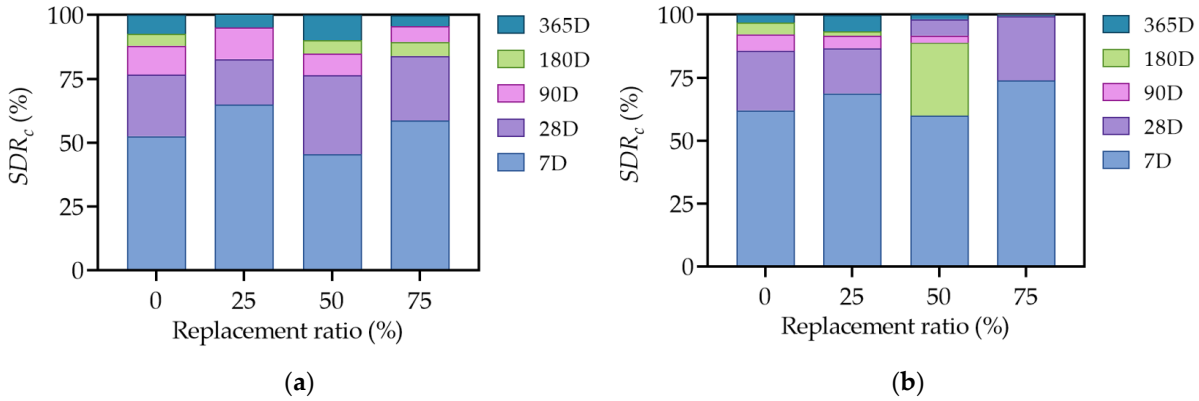

Figure 9. Strength development ratio of compressive strength (SDR_c) according to WOSP replacement ratio and cured at (**a**) tap water condition and (**b**) seawater condition.

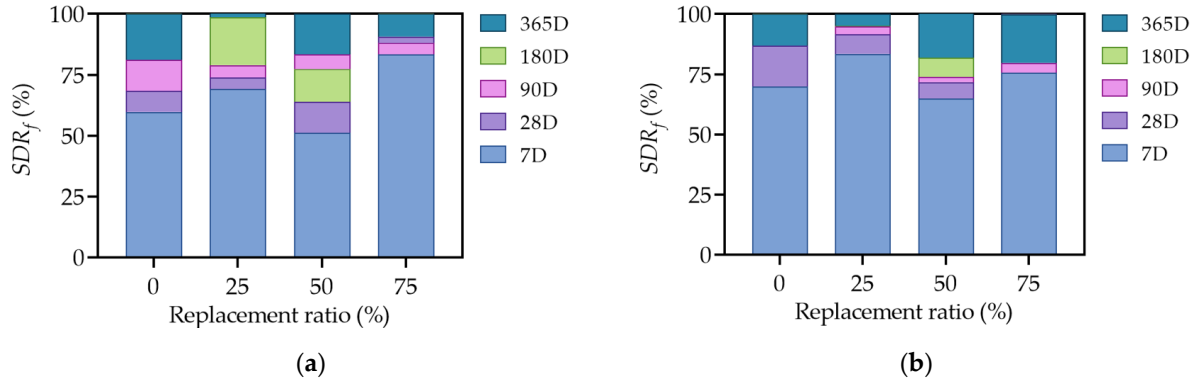

Figure 10. Strength development ratio of flexural strength (SDR_f) according to WOSP replacement ratio and cured at (**a**) tap water condition and (**b**) seawater condition.

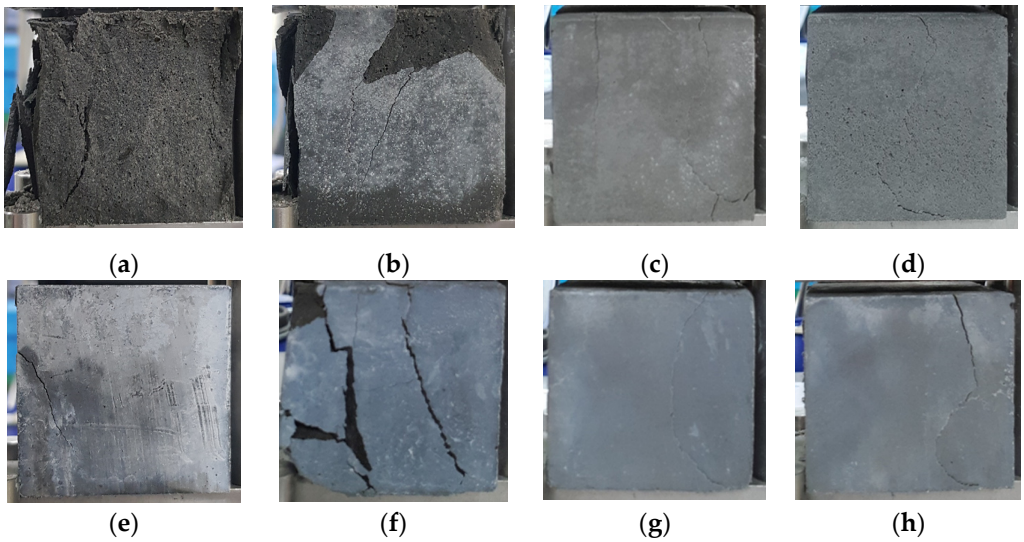

Figure 11. Failure modes of representative cubical samples: (**a**) W0-TW-28D; (**b**) W25-TW-28D; (**c**) W50-TW-28D; (**d**) W75-TW-28D; (**e**) W0-SW-28D; (**f**) W25-SW-28D; (**g**) W50-SW-28D; and (**h**) W75-SW-28D.

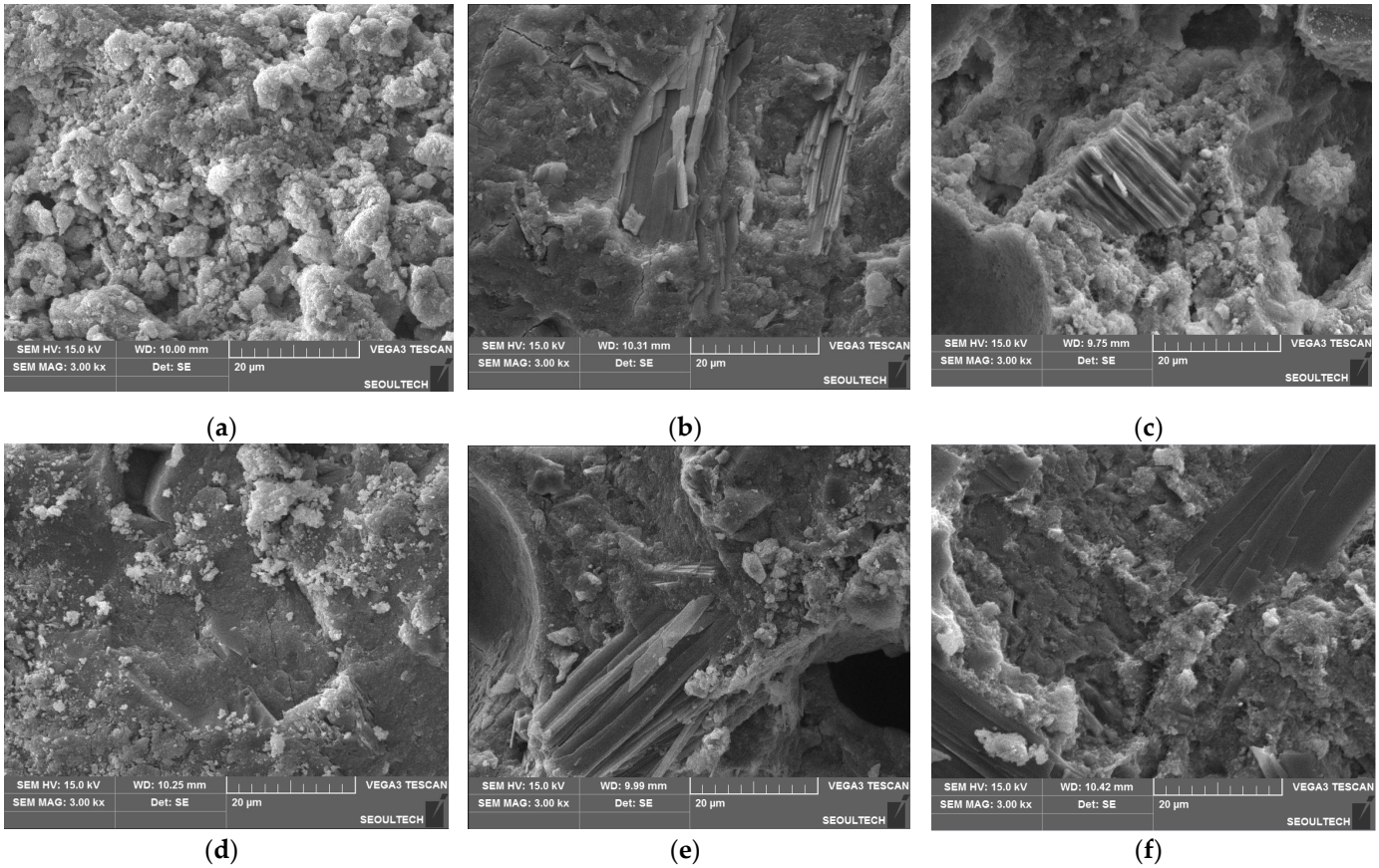

Figure 12. SEM images of representative samples: (**a**) W0-TW-28D; (**b**) W25-TW-28D; (**c**) W75-TW-28D; (**d**) W0-SW-28D; (**e**) W25-SW-28D; and (**f**) W75-SW-28D.

5.2. Effect of Curing Water on the Strength and Microstructures of Cementitious Composites

Table 5 summarizes the results of the statistical analysis using ANOVA, confirming that there was no significant difference between the strengths of the samples exposed to different curing water conditions. Specifically, the F-statistic for the compressive strength was 0.086, which was not significant at a significance level of 0.05. This indicates that there was no statistically significant difference between the compressive strengths under the two water conditions. A *p*-value of 0.770 further supports this conclusion. Similarly, for the flexural strength, the F-statistic was 0.454 with a *p*-value of 0.501, indicating no significant difference between the measured values, as summarized in Table 5. However, the effect of different curing waters on compressive strength development was confirmed only in the early stages. For example, at 7 and 28 d, the mean compressive strengths of the seawater-cured samples were 8.8% and 4.8% higher than those of the tap-water-cured samples, respectively. However, the effect of seawater on the development of compressive strength diminished after 90 d. For example, the compressive strength development of samples cured in seawater reached only 56% of that of samples cured in tap water. A similar trend was observed for the measured mean flexural strength values at 7 and 28 d. These results may be attributed to the presence of some ions such as chloride and sulfate in seawater, which accelerates the rate of cement hydration as pointed out by previous studies [64–67]. Consequently, faster material setting and initial strength gain were observed regardless of the WOSP content. This trend is also consistent with previous studies that indicated the effect of seawater on early strength gain [68,69].

Table 5. ANOVA test results for all compressive and flexural strength values of samples cured under different water conditions.

Compressive Strength (MPa)						
Groups	Count	Sum		Average		Variance
TW	100	2305.8		23.06		177.812
SW	100	2252.6		22.53		152.62
Source of Variation	SS	df	MS	*F*	*p*-value	*F* crit.
Between groups	14.1	1	14.12	0.0855	0.7703	3.88885
Within groups	32,712.8	198	165.22			
Total	32,726.9	199				
Flexural Strength (MPa)						
Groups	Count	Sum		Average		Variance
TW	100	491.5		4.91		5.949
SW	100	515.3		5.15		6.529
Source of Variation	SS	df	MS	*F*	*p*-value	*F* crit.
Between groups	2.8	1	2.83	0.454	0.5012	3.88885
Within groups	1235.3	198	6.24			
Total	1238.1	199				

Figure 13 shows the XRD patterns of the representative samples (TW-7D, SW-7D, TW-28D, and SW-28D) cured under different water conditions for 7 and 28 d. $CaCO_3$, a component that forms C–S–H bonds, was observed at approximately 30°, whereas SiO_2 appeared at approximately 26.5° in substantial quantities. The XRD analysis revealed that most samples prepared with WOSP contained $CaCO_3$, and the peak of $CaCO_3$ tended to increase with an increasing WOSP replacement ratio, as depicted in Figure 13. Conversely, the control samples showed a peak of SiO_2 at 26.5° with less $CaCO_3$ compared with that in the WOSP samples. Furthermore, the 50 and 75% WOSP replacement groups exhibited similar trends in their XRD patterns, regardless of the curing period. This may be attributed to the slow pozzolanic reaction caused by the excessive amount of WOSP.

The results of XRD patterns for the reference samples are in good agreement with previous studies, revealing the presence of ettringite, portlandite, calcium carbonate hydrate, aluminate, and quartz [70,71]. This finding is consistent with the reported preferential formation of hemicarbonate in the presence of calcium carbonate [70]. All samples exhibited peaks associated with hydration and carbonation products. The intensity of peaks corresponding to unhydrated clinker minerals like alite and belite was lower, as expected [71].

Seawater exposure was expected to contribute to the formation of ettringite, gypsum, brucite, and the peak of Friedel's salt due to the presence of ions like SO_4^{2-}, Mg^{2+}, and Cl^- [40]. Further investigation using fractal analysis and thermodynamic methods might be necessary to understand the changes in the hydration process and microstructure of cementitious composites containing WOSP [72–75]. Overall, it can be concluded that the WOSP replacement ratio has a significant influence on the strength development and microstructural changes than the curing water type. However, long-term investigations on weight loss, mass change, and pore structure using thermogravimetric analysis and MIP are necessary.

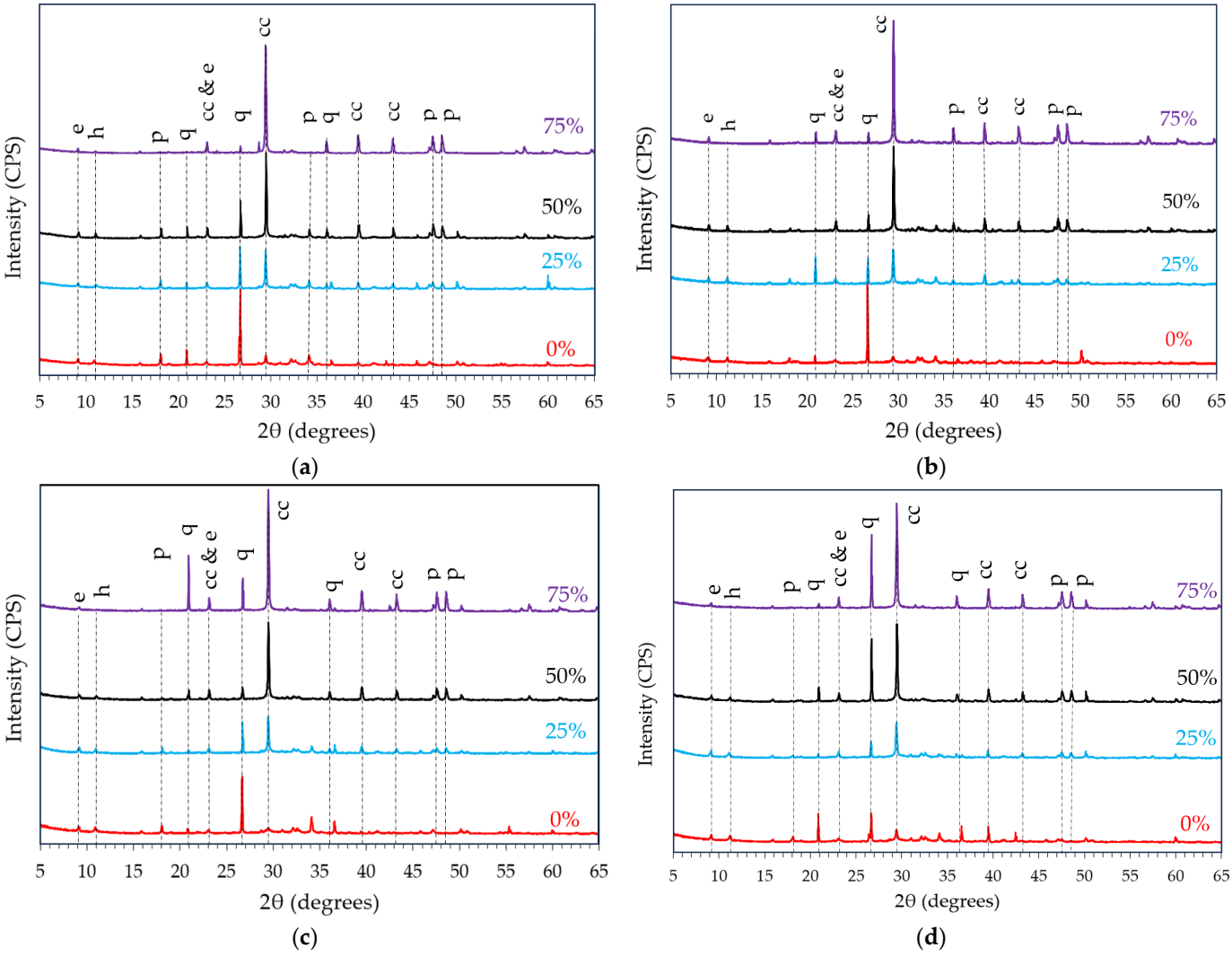

Figure 13. XRD patterns of representative samples: (**a**) TW-7D; (**b**) SW-7D; (**c**) TW-28D; and (**d**) SW-28D. cc = calcium carbonate; e = ettringite; h = hemicarboaluminate; p = portlandite; q = quartz.

5.3. Effect of Curing Periods on the Strength and Microstructures of Cementitious Composites

The strength changes were examined between the ages of 7 and 365 d. The mean values gradually increased, demonstrating a strong correlation with the WOSP replacement ratio. For instance, the mean compressive strength increased by 84% and 52% between 7 and 365 d under the TW and SW conditions, respectively. Similarly, the mean flexural strength increased by 57% and 37% under the same conditions. The samples cured under conventional water conditions exhibited higher strength values than those cured in SW. However, some samples exposed to SW exhibited early-age strength gain, although its impact was restricted to the early stages.

It can be concluded that the curing period influences the strength development, whereas the rate of increase is affected by a combination of other test variables. Notably, no substantial strength gain was observed after 28 d. The mean compressive strength changes in the samples cured under TW and SW conditions were modest, reaching only 10% and 6%, respectively, between 90 and 365 d, except for the W75-SW group. Moreover, for the samples with a 25% WOSP replacement ratio, the strength changes were negligible, regardless of the curing period. This finding aligns with the findings of previous research [33,34]. This implies that strength measurements at 28 d may be sufficient to assess the effectiveness of WOSP as a cement replacement.

The microstructural changes in the WOSP samples were investigated only during the early stages. Tricalcium silicate (C_3S) is generally considered the most reactive component contributing to early strength development and the hydration process of cement. While also reactive, tricalcium aluminate (C_3A) tends to contribute more to the initial setting and early strength development. Additionally, it can be associated with certain types of early hydration issues, such as flash setting or rapid stiffening of cement [76,77]. This was the rationale for selecting the testing period for microstructural changes. However, further studies on the long-term microstructural changes are required.

6. Discussion

In this study, we examined the effects of various WOSP replacement ratios, curing water types, and curing durations on the mechanical properties and microstructures of cement mortars produced using WOSP as a cement replacement. However, further research is required for the efficient use of WOSP as a cement replacement material. Comprehensive research across multiple disciplines is essential for the wider adoption of WOSP in cementitious composites.

First, in-depth material characterization, such as analysis of WOSP's chemical composition (including calcium carbonate content and trace elements) and particle size distribution, is essential. Therefore, it is necessary to assess its impact on the workability and strength of concrete. Subsequently, researchers should focus on optimizing the mix design, determining the ideal percentage of WOSP, and determining its effect on the water-to-cement ratio. We confirmed that a WOSP replacement ratio higher than 25% should not be used because it can negatively influence the strength development and durability. The mechanical properties, including compressive, flexural, and tensile strengths, should be evaluated to ensure that the concrete meets the required standards. Durability performance, such as corrosion resistance and freeze–thaw resistance, is also crucial, particularly in concrete structures exposed to marine environments. Economic viability and environmental impact assessments along with compatibility studies with other admixtures are integral.

In addition, the specific surface area (SSA) of waste oyster shell powder (WOSP) is expected to significantly affect the mechanical properties of cementitious composites. WOSP with a high SSA and a regular particle shape can effectively enhance properties such as strength, stiffness, and durability when used as a replacement material in cementitious composites [39,49,78]. This enhancement is attributed to the increased reactivity and nucleation sites provided by the high SSA of WOSP, leading to improved hydration and densification of the cementitious matrix. A higher SSA of WOSP also implies that smaller quantities of the material are required to achieve the same desired effects compared with WOSP with a lower SSA. This efficiency in material usage translates to reduced costs and waste production, making WOSP a sustainable and economically viable alternative in cementitious composites.

In this study, the effects of three limited test variables on the strength development and microstructural changes in cementitious composites were experimentally investigated under controlled laboratory conditions. However, this study is part of an ongoing research project focusing on recycling WOSP in marine concrete structures, in applications such as floating renewable energy systems, breakwaters, and artificial reefs. Thus, field trials are imperative to validate laboratory findings, and long-term monitoring of concrete structures built with WOSP is essential for assessing durability over time.

7. Conclusions

In this study, the effect of the addition of waste oyster shell powder (WOSP) on the strength development and microstructural changes in cementitious composites exposed to two different water conditions for 7–365 d was experimentally examined. The measured compressive strength, flexural strength, sorptivity, SEM, and XRD results were analyzed, and the following conclusions were drawn:

(1) A WOSP replacement ratio higher than 25% negatively influenced strength development, and reduced reactivity was observed based on the SEM and XRD results.
(2) The effect of different curing waters on compressive strength development was confirmed only in the early stages, potentially related to the presence of chloride in seawater, which accelerates the rate of cement hydration.
(3) The mean strength values gradually increased between 7 and 365 d, with no substantial strength gain beyond 28 d.
(4) The stronger correlations were observed between the compressive strength and initial sorptivity, with higher R values in comparison with the flexural strength.
(5) The XRD analysis revealed that most samples prepared with WOSP contained $CaCO_3$, and the peak of $CaCO_3$ tended to increase with an increasing WOSP replacement ratio.
(6) The SEM results revealed that a high replacement ratio of WOSP can have a negative influence on cement hydration and the pozzolanic effect.

Overall, the WOSP replacement ratio exhibited a dominant effect on both the strength and microstructure compared with the other variables. Further studies are necessary to examine the long-term changes in the microstructures. Because this study is part of an ongoing research project focusing on recycling WOSP in marine concrete structures, the limitations highlighted herein are further examined and reported.

Author Contributions: Conceptualization, M.O.K.; methodology, M.O.K.; software, M.O.K.; validation, M.K.L. and M.O.K.; formal analysis, M.K.L. and M.O.K.; investigation, M.K.L. and M.O.K.; resources, M.K.L.; data curation, M.O.K.; writing—original draft preparation, M.O.K.; writing—review and editing, M.O.K.; visualization, M.O.K.; supervision, M.K.L.; project administration, M.O.K.; funding acquisition, M.O.K. All authors have read and agreed to the published version of the manuscript.

Funding: This study was financially supported by Seoul National University of Science & Technology.

Data Availability Statement: Available upon request to the corresponding author.

Acknowledgments: The authors express sincere gratitude to Seoul National University of Science & Technology for the financial support.

Conflicts of Interest: The authors declare no conflict of interest.

Appendix A

Table A1. Compressive strength values of cementitious composites containing various waste shell powders [41,42].

Classification	Type of Cement	*w*/*c* Ratio, Cement to Sand Ratio * (%)	Replacement Ratio (%)	Compressive Strength (28 days, MPa)	Reference
Cockle	Type I Ordinary Portland cement	35.51 (*w*/*c*)	0.0 2.0 4.0 6.0 8.0	36.20 30.84 32.24 28.86 30.56	Olivia et al. [43]
Oyster	Type I Ordinary Portland cement	1:4 *	0.0 5.0 10.0 15.0 20.0	7.50 to 15.00	Lertwattanaruk et al. [44]
Cockle	Ordinary Portland cement	35.82 (*w*/*c*)	0.0 4.0	38.00 36.00	Olivia et al. [45]

Table A1. *Cont.*

Classification	Type of Cement	*w/c* Ratio, Cement to Sand Ratio * (%)	Replacement Ratio (%)	Compressive Strength (28 days, MPa)	Reference
Clam	Ordinary Portland cement	35.82 (w/c)	0.0 4.0	38.00 39.00	Olivia et al. [45]
Oyster	Ordinary Portland cement	40.00 (w/b)	0.0 2.5 5.0 7.5 10.0	38.00 40.00 42.00 40.00 39.50	Abinaya et al. [46]
Oyster	Ordinary Portland cement	-	5.0	5% increased	Zhong et al. [47]
Oyster	Ordinary Portland cement	-	5.0 to 20.0	Up to 35% decreased	Zhong et al. [47]
Oyster	Ordinary Portland cement (CEM I 52.5)	40.00 (w/c)	0.0 8.0 16.0 33.0	60.30 50.00 to 57.50 37.50 to 52.50 27.50 to 42.50	Ez-zaki et al. [48]

* Cement to sand ratio.

References

1. Andrew, R.M. Global CO_2 Emissions from Cement Production, 1928–2018. *Earth Syst. Sci. Data* **2019**, *11*, 1675–1710. [CrossRef]
2. A Plaza, M.G.; Martínez, S.; Rubiera, F. CO_2 Capture, Use, and Storage in the Cement Industry: State of the Art and Expectations. *Energies* **2020**, *13*, 5692. [CrossRef]
3. Liao, Y.; Yao, J.; Deng, F.; Li, H.; Wang, K.; Tang, S. Hydration behavior and strength development of supersulfated cement prepared by calcined phosphogypsum and slaked lime. *J. Build. Eng.* **2023**, *80*, 108075. [CrossRef]
4. Aamar Danish, M.; Usama Salim, T.A. Trends and Developments in Green Cement "A Sustainable Approach". *Sustain. Struct. Mater.* **2019**, *2*, 45–60.
5. Imbabi, M.S.; Carrigan, C.; McKenna, S. Trends and Developments in Green Cement and Concrete Technology. *Int. J. Sustain. Built Environ.* **2012**, *1*, 194–216. [CrossRef]
6. Tang, S.; Cai, R.; He, Z.; Cai, X.; Shao, H.; Li, Z.; Yang, H.; Chen, E. Continuous microstructural correlation of slag/superplasticizer cement pastes by heat and impedance methods via fractal analysis. *Fractals* **2017**, *25*, 1740003. [CrossRef]
7. Mach, K.; Mastrandrea, M. *Climate Change 2014: Impacts, Adaptation, and Vulnerability*; Cambridge University Press: Cambridge, UK, 2014; Volume 1.
8. Alshammari, Y.M. Achieving Climate Targets via the Circular Carbon Economy: The Case of Saudi Arabia. *C J. Carbon Res.* **2020**, *6*, 54. [CrossRef]
9. Van Der Zwaan, B.; Smekens, K. CO_2 Capture and Storage with Leakage in an Energy-Climate Model. *Environ. Model. Assess.* **2009**, *14*, 135–148. [CrossRef]
10. Tang, L.; Ruan, J.H.; Bo, X.; Mi, Z.F.; Wang, S.Y.; Dong, G.X.; Davis, S.J. Plant-level real-time monitoring data reveal substantial abatement potential of air pollution and CO_2 in China's cement sector. *One Earth* **2022**, *5*, 892–906. [CrossRef]
11. Li, H.; Tan, X.C.; Guo, J.X.; Zhu, K.W.; Huang, C. Study on an Implementation Scheme of Synergistic Emission Reduction of CO_2 and Air Pollutants in China's Steel Industry. *Sustainability* **2019**, *11*, 352. [CrossRef]
12. Kim, H.S.; Kasipandi, S.; Kim, J.; Kang, S.H.; Kim, J.H.; Ryu, J.H.; Bae, J.W. Current Catalyst Technology of Selective Catalytic Reduction (SCR) for NOx Removal in South Korea. *Catalysts* **2020**, *10*, 52. [CrossRef]
13. Seo, J.H.; Kim, Y.J.; Cho, K.H.; Cho, J.S.; Han, K.H.; Yoon, D.Y. Trend of Nitrogen Oxide Reduction Technologies in Cement Industry. *J. Korean Inst. Resour. Recycl.* **2020**, *29*, 114–124. [CrossRef]
14. Rivera, F.; Martínez, P.; Castro, J.; López, M.; Rivera, F.; Martínez, P.; Castro, J.; López, M. Massive volume fly-ash concrete: A more sustainable material with fly ash replacing cement and aggregates. *Cem. Concr. Compos.* **2015**, *63*, 104–112. [CrossRef]
15. Wang, L.; Huang, Y.; Zhao, F.; Huo, T.; Chen, E.; Tang, S. Comparison between the influence of finely ground phosphorous slag and fly ash on frost resistance, pore structures and fractal features of hydraulic concrete. *Fractal Fract.* **2022**, *6*, 598. [CrossRef]
16. Błaszczyński, T.; Król, M. Usage of Green Concrete Technology in Civil Engineering. *Procedia Eng.* **2015**, *122*, 296–301. [CrossRef]
17. Müller, H.S.; Haist, M.; Vogel, M. Assessment of the sustainability potential of concrete and concrete structures considering their environmental impact, performance and lifetime. *Constr. Build. Mater.* **2014**, *67*, 321–337. [CrossRef]
18. Gilfillan, D.; Marland, G. CDIAC-FF: Global and national CO_2 emissions from fossil fuel combustion and cement manufacture: 1751–2017. *Earth Syst. Sci. Data* **2021**, *13*, 1667–1680. [CrossRef]
19. Susmitha, P.J.R.L.P.; Rao, M.K. Comparative study on strength and durability of concrete upon partial substitution of fly ash and bagasse ash in conventional concrete. *IOP Conf. Ser. Earth Environ. Sci.* **2022**, *982*, 012011. [CrossRef]

20. Xu, G.; Shi, X. Characteristics and applications of fly ash as a sustainable construction material: A state-of-the-art review. *Resour. Conserv. Recycl.* **2018**, *136*, 95–109. [CrossRef]
21. Awoyera, P.O.; Akinmusuru, J.O.; Ndambuki, J.M. Green concrete production with ceramic wastes and laterite. *Constr. Build. Mater.* **2016**, *117*, 29–36. [CrossRef]
22. Chen, W.; Jin, R.; Xu, Y.; Wanatowski, D.; Li, B.; Yan, L.; Pan, Z.; Yang, Y. Adopting recycled aggregates as sustainable construction materials: A review of the scientific literature. *Constr. Build. Mater.* **2019**, *218*, 483–496. [CrossRef]
23. Çelik, Z.; Bingöl, A.F.; Ağsu, A.S. Fresh, mechanical, sorptivity and rapid chloride permeability properties of self-compacting concrete with silica fume and fly ash. *Iran. J. Sci. Technol. Trans. Civ. Eng.* **2022**, *46*, 789–799. [CrossRef]
24. Yang, K.-H.; Jung, Y.-B.; Cho, M.-S.; Tae, S.-H. Effect of supplementary cementitious materials on reduction of CO_2 emissions from concrete. *J. Clean. Prod.* **2015**, *103*, 774–783. [CrossRef]
25. Al-Gahtani, K.; Alsulaihi, I.; Ali, M.; Marzouk, M. Production of green concrete using recycled waste aggregate and byproducts. *Built Environ. Proj. Asset Manag.* **2017**, *7*, 413–425. [CrossRef]
26. Berndt, M.L. Properties of sustainable concrete containing fly ash, slag and recycled concrete aggregate. *Constr. Build. Mater.* **2009**, *23*, 2606–2613. [CrossRef]
27. Sadek, D.M.; El-Attar, M.M. Development of high-performance green concrete using demolition and industrial wastes for sustainable construction. *J. Am. Sci.* **2012**, *8*, 120–131.
28. Choi, S.H.; Lee, J.H.; Yoo, J.; Park, J.H.; Bae, J.S.; Park, C.Y. Toward transformation of bivalve shell wastes into high value-added and sustainable products in South Korea: A review. *J. Ind. Eng. Chem.* 2023; *in press*. [CrossRef]
29. Lee, C.H.; Lee, D.K.; Ali, M.A.; Kim, P.J. Effects of oyster shell on soil chemical and biological properties and cabbage productivity as a liming materials. *Waste Manag.* **2008**, *28*, 2702–2708. [CrossRef] [PubMed]
30. Ok, Y.S.; Lim, J.E.; Moon, D.H. Stabilization of Pb and Cd contaminated soils and soil quality improvements using waste oyster shells. *Environ. Geochem. Health* **2011**, *33*, 83–91. [CrossRef]
31. Çatli, A.U.; Bozkurt, M.; Küçükyilmaz, K.; Çinar, M.; Bintas, E.; Çöven, F.; Atik, H. Performance and egg quality of aged laying hens fed diets supplemented with meat and bone meal or oyster shell meal. *S. Afr. J. Anim. Sci.* **2012**, *42*, 74–82. [CrossRef]
32. Osorio-López, C.; Seco-Reigosa, N.; Garrido-Rodríguez, B.; Cutillas-Barreiro, L.; Arias-Estévez, M.; Fernández-Sanjurjo, M.J.; Álvarez-Rodríguez, E.; Núñez-Delgado, A. As(V) adsorption on forest and vineyard soils and pyritic material with or without mussel shell: Kinetics and fractionation. *J. Taiwan Inst. Chem. Eng.* **2014**, *45*, 1007–1014. [CrossRef]
33. Yang, E.I.; Yi, S.T.; Leem, Y.M. Effect of oyster shell substituted for fine aggregate on concrete characteristics: Part I. fundamental properties. *Cem. Concr. Res.* **2005**, *35*, 2175–2182. [CrossRef]
34. Yang, E.-I.; Kim, M.-Y.; Park, H.-G.; Yi, S.-T. Effect of partial replacement of sand with dry oyster shell on the long-term performance of concrete. *Constr. Build. Mater.* **2010**, *24*, 758–765. [CrossRef]
35. Kuo, W.-T.; Wang, H.-Y.; Shu, C.-Y.; Su, D.-S. Engineering properties of controlled low-strength materials containing waste oyster shells. *Constr. Build. Mater.* **2013**, *46*, 128–133. [CrossRef]
36. Liu, R.; Fan, J.; Yu, X.; Zhu, Y.; Chen, D. Properties of mortar containing polyvinyl alcohol pretreated waste oyster shells with various concentrations. *Constr. Build. Mater.* **2023**, *363*, 129879. [CrossRef]
37. Bamigboye, G.O.; Nworgu, A.T.; Odetoyan, A.O.; Kareem, M.; Enabulele, D.O.; Bassey, D.E. Sustainable use of seashells as binder in concrete production: Prospect and challenges. *J. Build. Eng.* **2021**, *34*, 101864. [CrossRef]
38. Soltanzadeh, F.; Emam-Jomeh, M.; Edalat-Behbahani, A.; Soltanzadeh, Z. Development and characterization of blended cements containing seashell powder. *Constr. Build. Mater.* **2018**, *161*, 292–304. [CrossRef]
39. Han, Y.; Lin, R.; Wang, X.Y. Performance of sustainable concrete made from waste oyster shell powder and blast furnace slag. *J. Build. Eng.* **2022**, *47*, 103918. [CrossRef]
40. Seifu, M.N.; Park, J.K.; Han, T.H.; Park, S.; Kim, M.O. Effect of oyster shell powder addition on hydration of Portland cement-calcium sulfoaluminate cement-blast furnace slag or-metakaolin ternary cement. *Case Stud. Constr. Mater.* **2022**, *17*, e01529. [CrossRef]
41. Tayeh, B.A.; Hasaniyah, M.W.; Zeyad, A.M.; Yusuf, M.O. Properties of concrete containing recycled seashells as cement partial replacement: A review. *J. Clean. Prod.* **2019**, *237*, 117723. [CrossRef]
42. Mo, K.H.; Alengaram, U.J.; Jumaat, M.Z.; Lee, S.C.; Goh, W.I.; Yuen, C.W. Recycling of seashell waste in concrete: A review. *Constr. Build. Mater.* **2018**, *162*, 751–764. [CrossRef]
43. Olivia, M.; Mifshella, A.A.; Darmayanti, L. Mechanical properties of seashell concrete. *Procedia Eng.* **2015**, *125*, 760–764. [CrossRef]
44. Lertwattanaruk, P.; Makul, N.; Siripattarapravat, C. Utilization of ground waste seashells in cement mortars for masonry and plastering. *J. Environ. Manag.* **2012**, *111*, 133–141. [CrossRef]
45. Olivia, M.; Oktaviani, R. Properties of concrete containing ground waste cockle and clam seashells. *Procedia Eng.* **2017**, *171*, 658–663. [CrossRef]
46. Abinaya, S.; Venkatesh, S.P. An effect on oyster shell powder's mechanical properties in self compacting concrete. *Int. J. Innov. Res. Sci. Eng. Tech.* **2016**, *5*, 11785–11789.
47. Zhong, B.Y.; Zhou, Q.; Chan, C.F.; Yu, Y. Structure and property characterization of oyster shell cementing material. *Jiegou Huaxue* **2012**, *31*, 85–92.
48. Ez-Zaki, H.; Diouri, A.; Kamali-Bernard, S.; Sassi, O. Composite Cement Mortars Based on Marine Sediments and Oyster ShellPowder. *Mater. Constr.* **2016**, *66*, e080. [CrossRef]

49. Liu, S.; Wang, Y.; Liu, B.; Zou, Z.; Teng, Y.; Ji, Y.; Zhou, Y.; Zhang, L.V.; Zhang, Y. Sustainable Utilization of Waste Oyster Shell Powders with Different Fineness Levels in a Ternary Supplementary Cementitious Material System. *Sustainability* **2022**, *14*, 5981. [CrossRef]
50. Liao, Y.; Fan, J.; Li, R.; Da, B.; Chen, D.; Zhang, Y. Influence of the Usage of Waste Oyster Shell Powder on Mechanical Properties and Durability of Mortar. *Adv. Powder Technol.* **2022**, *33*, 103503. [CrossRef]
51. Chen, D.; Zhang, P.; Pan, T.; Liao, Y.; Zhao, H. Evaluation of the eco-friendly crushed waste oyster shell mortars containing supplementary cementitious materials. *J. Clean. Prod.* **2019**, *237*, 117811. [CrossRef]
52. Kong, J.; Cong, G.; Ni, S.; Sun, J.; Guo, C.; Chen, M.; Quan, H. Recycling of waste oyster shell and recycled aggregate in the porous ecological concrete used for artificial reefs. *Constr. Build. Mater.* **2022**, *323*, 126447. [CrossRef]
53. Klathae, T. Utilization of Crushed Oyster Shell on Interlocking Black. *RMUTP Res. J.* **2017**, *11*, 167–177.
54. Xu, Q.Z.; Zhang, L.B.; Zhang, T.; Zhou, Y.; Xia, S.D.; Liu, H.; Yang, H.S. Effects of an artificial oyster shell reef on macrobenthic communities in Rongcheng Bay, East China. Chin. *J. Oceanol. Limnol.* **2014**, *32*, 99–110. [CrossRef]
55. Choi, S.I.; Kil Park, J.; Han, T.H.; Pae, J.; Moon, J.; Kim, M.O. Early-age mechanical properties and microstructures of Portland cement mortars containing different admixtures exposed to seawater. *Case Stud. Constr. Mater.* **2022**, *16*, e01041. [CrossRef]
56. Park, S.; Park, J.K.; Lee, N.; Kim, M.O. Exploring Structural Evolution of Portland Cement Blended with Supplementary Cementitious Materials in Seawater. *Materials* **2021**, *14*, 1210. [CrossRef] [PubMed]
57. *ASTM C109/C109M*; Standard Test Method for Compressive Strength of Hydraulic Cement Mortars (Using 2-in. or [50-Mm] Cube Specimens). American Society for Testing and Materials: West Conshohocken, PA, USA, 2020.
58. *ASTM C348*; Standard Test Method for Flexural Strength of Hydraulic-Cement Mortars1. ASTM International: West Conshohocken, PA, USA, 1998.
59. *ASTM C1585-20*; Standard Test Method for Measurement of Rate of Absorption of Water by Hydraulic-Cement Concretes. ASTM International: West Conshohocken, PA, USA, 2020.
60. *ACI 363 R-10*; Report on High-Strength Concrete. American Concrete Institute: Farmington Hills, MI, USA, 2010.
61. *CEB-FIP MC 90*; Design of Concrete Structures. CEB-FIP Model Code 1990. Thomas Telford: London, UK, 1993.
62. Wu, H.; Xie, Z.; Zhang, L.; Lin, Z.; Wang, S.; Tang, W. A New Magnesium Phosphate Cement Based on Renewable Oyster Shell Powder: Flexural Properties at Different Curing Times. *Materials* **2021**, *14*, 5433. [CrossRef] [PubMed]
63. Cha, I.; Kim, J.; Lee, H. Enhancing Compressive Strength in Cementitious Composites through Effective Use of Wasted Oyster Shells and Admixtures. *Buildings* **2023**, *13*, 2787. [CrossRef]
64. Li, Y.; Zhang, H.; Huang, M.H.; Yin, H.B.; Jiang, K.; Xiao, K.T.; Tang, S.W. Influence of Different Alkali Sulfates on the Shrinkage, Hydration, Pore Structure, Fractal Dimension and Microstructure of Low-Heat Portland Cement, Medium-Heat Portland Cement and Ordinary Portland Cement. *Fractal Fract.* **2021**, *5*, 79. [CrossRef]
65. Qu, F.; Li, W.; Wang, K.; Tam, V.W.Y.; Zhang, S. Effects of seawater and undesalted sea sand on the hydration products, mechanical properties and microstructures of cement mortar. *Constr. Build. Mater.* **2021**, *310*, 125229. [CrossRef]
66. Li, Q.; Geng, H.; Shui, Z.; Huang, Y. Effect of metakaolin addition and seawater mixing on the properties and hydration of concrete. *Appl. Clay Sci.* **2015**, *115*, 51–60. [CrossRef]
67. Zhang, M.; Chen, J.; Lv, Y.; Wang, D.; Ye, J. Study on the expansion of concrete under attack of sulfate and sulfate–chloride ions. *Constr. Build. Mater.* **2013**, *39*, 26–32. [CrossRef]
68. Mohammed, T.U.; Hamada, H.; Yamaji, T. Performance of seawater-mixed concrete in the tidal environment. *Cem. Concr. Res.* **2004**, *34*, 593–601. [CrossRef]
69. Wegian, F.M. Effect of seawater for mixing and curing on structural concrete. *IES J. Part A Civ. Struct. Eng.* **2010**, *3*, 235–243. [CrossRef]
70. Matschei, T.; Lothenbach, B.; Glasser, F.P. The role of calcium carbonate in cement hydration. *Cem. Concr. Res.* **2007**, *37*, 551–558. [CrossRef]
71. Seo, J.H.; Park, S.M.; Yang, B.J.; Jang, J.G. Calcined Oyster Shell Powder as an Expansive Additive in Cement Mortar. *Materials* **2019**, *12*, 1322. [CrossRef] [PubMed]
72. Santhanam, M.; Cohen, M.; Olek, J. Differentiating seawater and groundwater sulfate attack in Portland cement mortars. *Cem. Concr. Res.* **2006**, *36*, 2132–2137. [CrossRef]
73. Yang, H.M.; Zhang, S.M.; Lei, W.; Chen, P.; Shao, D.K.; Tang, S.W.; Li, J.Z. High-ferrite Portland cement with slag: Hydration, microstructure, and resistance to sulfate attack at elevated temperature. *Cement Concrete Comp.* **2022**, *130*, 104560. [CrossRef]
74. Huang, J.; Li, W.; Huang, D.; Wang, L.; Chen, E.; Wu, C.; Wang, B.; Deng, H.; Tang, S.; Shi, Y.; et al. Fractal Analysis on Pore Structure and Hydration of Magnesium Oxysulfate Cements by First Principle, Thermodynamic and Microstructure-Based Methods. *Fractal Fract.* **2021**, *5*, 164. [CrossRef]
75. Peng, Y.; Tang, S.; Huang, J.; Tang, C.; Liu, Y. Fractal analysis on pore structure and modeling of hydration of magnesium phosphate cement paste. *Fractal Fract.* **2022**, *6*, 337. [CrossRef]
76. Zhou, Y.; Li, W.; Peng, Y.; Tang, S.; Wang, L.; Shi, Y.; Li, Y.; Wang, Y.; Geng, Z.; Wu, K. Hydration and Fractal Analysis on Low-Heat Portland Cement Pastes Using Thermodynamics-Based Methods. *Fractal Fract.* **2023**, *7*, 606. [CrossRef]

77. Tang, S.; Wang, Y.; Geng, Z.; Xu, X.; Yu, W.; Chen, J. Structure, Fractality, Mechanics and Durability of Calcium Silicate Hydrates. *Fractal Fract.* **2021**, *5*, 47. [CrossRef]
78. Bellei, P.; Torres, I.; Solstad, R.; Flores-Colen, I. Potential Use of Oyster Shell Waste in the Composition of Construction Composites: A Review. *Buildings* **2023**, *13*, 1546. [CrossRef]